Comparison of evaporation estimates from the REEM and EEFlux models in a shallow water body. Case: Bustillos Lake, Chihuahua, Mexico

Comparación de estimaciones de modelos de evaporación REEM y EEFlux en cuerpos de agua someros. Caso: Laguna de Bustillos, Chihuahua, México

Hugo Rojas-Villalobos[1], ORCID: https://orcid.org/0000-0002-2483-9228

Zohrab Samani[2], ORCID: https://orcid.org/0000-0002-3273-0599

Christopher Brown[3], ORCID: https://orcid.org/0000-0002-3622-6226

Luis Alatorre-Cejudo[4], ORCID: https://orcid.org/0000-0003-0837-3381

Blair Stringam[5], ORCID: https://orcid.org/0000-0003-3810-2152

Víctor Salas-Aguilar[6], ORCID: https://orcid.org/0000-0002-0258-7816

[1]Licenciatura en Geoinformática, Universidad Autónoma de Ciudad Juárez, Chihuahua, México, hlrojas@uacj.mx

[2]Civil Engineering, New Mexico State University, Las Cruces, NM, USA, zsamani@nmsu.edu

[3]Department of Geography, New Mexico State University, Las Cruces, NM, USA, brownchr@nmsu.edu

[4]Licenciatura en Geoinformática, Universidad Autónoma de Ciudad Juárez, Chihuahua, México, luis.alatorre@uacj.mx

[5]Plant and Environmental Sciences, New Mexico State University, Las Cruces, NM, USA, blairs@nmsu.edu

[6]Licenciatura en Geoinformática, Universidad Autónoma de Ciudad Juárez, Chihuahua, México, victor.salas@uacj.mx

Corresponding author: Hugo Rojas-Villalobos, hlrojas@uacj.mx

Abstract

Waterbody evaporation (E) within endorheic basins in semiarid areas is a critical factor in determining the water balance. Accurate E measurements can provide valuable information for the sustainable management of water resources in the face of climate change scenarios. However, evaporation can be estimated through methods as efficient as Penman using variables from agroclimatic stations, such as wind velocity, net radiation, relative humidity, and air temperature, which have a spatiotemporal variability. Within the evaporation models based on remote sensing (RS) is the surface energy balance model (SEB), which has been applied to different methodologies and extends the measurements of evapotranspiration (ET) at a regional level. SEB-based methodologies use physical principles with minimal weather data requirements to estimate ET. Hence, this article compares two methodologies that estimate evaporation using RS: The Regional

Evapotranspiration Estimate Model (REEM) and the Earth Engine Evapotranspiration Flux (EEFlux). Comparing ET measurements obtained from REEM and EEFlux for seven Landsat OLI scenes in the agriculture cycle of April to September applied against the simplified Penman equation showed that the REEM performed better (d=94%) than the EEFlux (d=68%) for the indicated period. Although the comparison of REEM and EEFlux shows accurate E measurements (REEM), gridded weather data (EEFlux) needs to improve, increasing the scale using local information.

Keywords: REEM, EEFlux, waterbody, lake, lake, evaporation, latent heat flux, evapotranspiration.

Resumen

La evaporación de cuerpos de agua (E) dentro de cuencas endorreicas en áreas semiáridas es un factor crítico para la determinación del balance hídrico. Mediciones precisas de E pueden proporcionar información valiosa para gestionar recursos hídricos sustentablemente ante los escenarios de cambio climático. Sin embargo, la evaporación puede estimarse a través de métodos tan eficientes como la ecuación simplificada de Penman (S-Penman) utilizando variables de estaciones agroclimáticas, como la velocidad del viento, la radiación neta, la humedad relativa y la temperatura del aire, que tienen una variabilidad espacio-temporal. Dentro de los modelos de evaporación basados en sensores remotos (RS) se encuentra el modelo de balance de energía de superficie (SEB), que se ha aplicado a diferentes metodologías y extiende las mediciones de

evapotranspiración (ET) a nivel regional. Las metodologías basadas en SEB utilizan principios físicos con requisitos mínimos de datos climáticos para estimar ET. Este artículo compara dos metodologías que estiman la evaporación utilizando RS: el Modelo de Estimación de Evapotranspiración Regional (REEM) y el Flujo de Evapotranspiración Earth Engine (EEFlux). La comparación de mediciones de ET obtenidas de REEM y EEFlux para siete escenas Landsat OLI en el ciclo agrícola de abril a septiembre de 2019, comparadas contra S-Penman mostró que REEM tuvo un mejor desempeño (d = 94%) que el EEFlux (d = 68%) para el período indicado. Aunque la comparación de REEM y EEFlux muestra mediciones precisas de E (REEM), es necesario mejorar los datos meteorológicos cuadriculados (EEFlux), aumentando la escala utilizando información local.

Palabras clave: REEM, EEFlux, cuerpo de agua, lago, laguna, evaporación, flujo de calor latente, evapotranspiración.

Introduction

The Bustillos Lake is the largest water body (~100 km2) in the Cuauhtemoc Valley (in Chihuahua, Mexico), which is in an endorheic basin (3 302 km2). The climate is semiarid, and agriculture is intensive. High competition for water resources among stakeholders (Díaz Caravantes, Bravo Peña, Alatorre Cejudo, & Sánchez Flores, 2014) has exerted high pressure on the aquifer. According to Mexican authorities, this phenomenon has caused the aquifer to be overexploited (Diario Oficial de la Federación, 2015). For this reason, farmers have made dams and ditches to divert and retain a small part of the tributary flows before it reaches Bustillos Lake. These practices, however, limit the source of water that supplies it. Like any water body, the Bustillos Lake is essential for its thermoregulatory climate function in the region as it absorbs heat fluxes and releases moisture (Rooney & Bornemann, 2013; Subin, Murphy, Li, Bonfils, & Riley, 2012). It is also ecologically important as a resting place for migratory waterbirds (Mireles & Mellink, 2017). Aquatic systems in semiarid areas are susceptible to drastic variations in water levels as they affect the aquatic life (Amado-Álvarez, Pérez Cutillas, Ramírez Valle, & Alarcón Cabañero, 2016) that feeds waterbirds. If the water bodies are not well managed, they could dry up and cause irreversible damage to the ecological environment. Some examples of environmental damage are the Aral Sea between Kazakhstan and Uzbekistan (Gross, 2017), Lake Chad in the borders of Niger, Nigeria, Cameroon, and Chad (Okpara, Stringer, Dougill, & Bila, 2015), and Lake Urmia in Iran (AghaKouchak *et al*., 2015). These water bodies are drying up because of the diversion of tributary rivers to agricultural fields, droughts, and upstream competition for water. The lake's evaporation data are required to establish

administrative water resource policies to avoid catastrophic scenarios and conserve the water balance in the Cuauhtemoc Basin.

Evapotranspiration (ET) is a process that combines the evaporation of water surfaces, soil moisture, and transpiration from vegetation (Erickson *et al*., 2008). Evaporation is part of ET, governed by aerodynamic and energy equations (Penman, 1948). Under this approach, it is possible to estimate the evaporation of a water body by calculating ET using remote sensing (RS) techniques. The most effective techniques for measuring evapotranspiration are lysimeters or eddy covariance flux stations (Hirschi, Michel, Lehner, & Seneviratne, 2017). Nevertheless, this type of equipment does not exist in the region due to its high cost. Because of this situation, it is necessary to explore emerging alternative methodologies for measuring ET. Rohwer (1931) developed evaporation coefficients (Kpan) for the evaporation pan method (U.S. Class A pan) for each month of the year. The problem with this approach is that the method used lakes in Colorado as research sites. These sites contained clear water, and the physical aspects of the metal pan container affected evaporation measurements (Fu, Charles, & Yu, 2009; Rayner, 2007). The Bustillos Lake has particular characteristics that make it different from other lakes; besides being a shallow lake, turbidity is high caused by suspended material content (Álvarez, Cutillas, Valle, & Cabañero, 2016; Amado-Alvarez *et al*., 2019). Radiation flux from the sun penetrates deep into the water column in clear water conditions, absorbing energy (Smith & Tyler, 1967). Under conditions of turbidity and low depth (<3 m) (Rojas-Villalobos, Alatorre-Cejudo, Stringman, Samani, & Brown, 2018), suspended particles on the surface layer scatter solar radiation.

Therefore, the water temperature increases resulting in more evaporation (Kirk, 1985). Under these conditions, it is impossible to apply pan evaporation coefficients since the physical characteristics change in each lake.

The classification of methods for calculating evaporation is daytime air temperature range such as that of Papadakis (Papadakis, 1965); air temperature and day length such as Hamon (Hamon, 1960), and Blaney-Criddle (Blaney & Criddle, 1957); solar radiation and the air temperature such as Jensen-Haise (Jensen & Haise, 1963), Makkink (Makkink, 1957), and Stephens-Stewart (Stephens & Stewart, 1963); heat flux and water vapor flux (combination) such as De Bruin-Keijman (De Bruin & Keijman, 1979), Penman (Penman, 1948), Brutsaert-Stricker (Brutsaert & Stricker, 1979), and De Bruin (De Bruin, 1978). Although these methods can offer good evaporation approximations, estimates are local at the point of the reference weather station.

Given this limitation, RS techniques expand measurements to the regional scale in a cost-effective way. There are different satellite-based methods established on physical relationships and theoretical foundations. Zhang, Kimball, & Running (2016) classified ET retrieval methods into eight groups: i) Penman-Monteith (PM) (Cleugh, Leuning, Mu, & Running, 2007; Li *et al.*, 2017); ii) Priestley-Taylor (PT) (Martínez Pérez, García-Galiano, Martin-Gorriz, & Baille, 2017); iii) water-carbon linkage (WCL)(Fisher *et al.*, 2018); iv) water balance (WB) (Reitz, Senay, & Sanford, 2017); v) maximum entropy production (MEP)(H. Wang, Tetzlaff, & Soulsby, 2017); vi) surface energy balance (SEB)(Senkondo,

Munishi, Tumbo, Nobert, & Lyon, 2019); vii) Ts-VI space (TVI) (Zhu, Jia, & Lv, 2019); and viii) empirical and other methods (EO). Each physical-theoretical basis reported by these groups has advantages and restrictions. For instance, PM models have a robust physical base, but on the other hand, the forcing of meteorological variables induces and propagates uncertainty in the evaporation estimate. The simplified PM model is the theoretical basis of PT as a primary governing equation by adding semiempirical equations. The estimations of the water-carbon linkage method use the advantages of carbon processes, which increases uncertainty in carbon fluxes caused by forcing climatological data. The MEP model is the base of the nonequilibrium thermodynamics theory, which requires few enforced climatological variables but requires continuous surface temperature measurements. The SEB models require minimum local weather data and RS but are susceptible to temperature deviations and need clear-sky conditions. TVI models have low-temperature sensitivity but require clear-sky conditions and oversimplify TVI space relationships. A weak theoretical base of empirical models does not make them a robust option for water management policies.

Within the SEB classification, there are two methodologies with a robust physical-theoretical base: the regional evapotranspiration estimate model (REEM) (Hewitt, Fernald, & Samani, 2018; Kıvrak, Bawazir, Samani, Steele, & Sönmez, 2019; A. Samani & Bawazir, 2015; Z. Samani, Bawazir, Bleiweiss, *et al*., 2007; Z. Samani, Skaggs, & Bleiweiss, 2005) and the Earth Engine Evapotranspiration Flux (EEFlux) (Allen *et al*., 2015; Ayyad, Al Zayed, Ha, & Ribbe, 2019), which is a version of mapping evapotranspiration at high resolution with internalized calibration

(METRIC) (Allen, Tasumi, & Trezza, 2007; Allen, Tasumi, Trezza, *et al*., 2007). REEM and METRIC use the same physical basis of Surface Energy Balance Algorithms for Land (SEBAL)(Bastiaanssen, Menenti, Feddes, & Holtslag, 1998; Bastiaanssen, Pelgrum, *et al.,* 1998) but with some differences to sensible heat flux (H) estimation and net radiation (Rn). EEFlux is an integration of the METRIC model in the Google Earth Engine platform. EEFlux uses Landsat satellite images, NLDAS and CFSv2 gridded weather data (the United States and rest of the world, respectively) for calibrating the METRIC model (Allen, Tasumi, & Trezza, 2007; Allen, Tasumi, Trezza, *et al*., 2007; Irmak *et al*., 2012). RS can estimate waterbodies' evaporation through the relationship with evapotranspiration calculated using meteorological data from weather stations.

The Lake Bustillos basin region is in a critical situation for the management of surface water. It is necessary to develop civil infrastructure that allows efficient surface water use. Knowing the lake's evaporation rates is essential to indirectly estimate the runoff and generate evaporation data required for the regional hydrological study. The local agroclimatic data in ET models based on RS reduces the evaporative fraction difference compared to those that use regional climate data grids to estimate evaporation in waterbodies. Due to the importance of monitoring evaporation to carry out responsible water management, this study establishes a starting base to evaluate which of the two ET models that use remote sensors is more suitable to measure E. The main objectives of this paper are (i) to calculate E for the lake using the S-Penman equation, (ii) to estimate E through REEM and

EEFLUX, and (ii) to compare the effectiveness and performance of the ET models against the simplified Penman (S-Penman) equation (Valiantzas, 2006). Geospatial (2D) quantification of evaporation using RS and ET models is a viable and suitable technique for managing regional water resources.

Materials and methods

The processes that integrate the methodology for comparing the performance of REEM and EEFlux with the S-Penman is as follows:
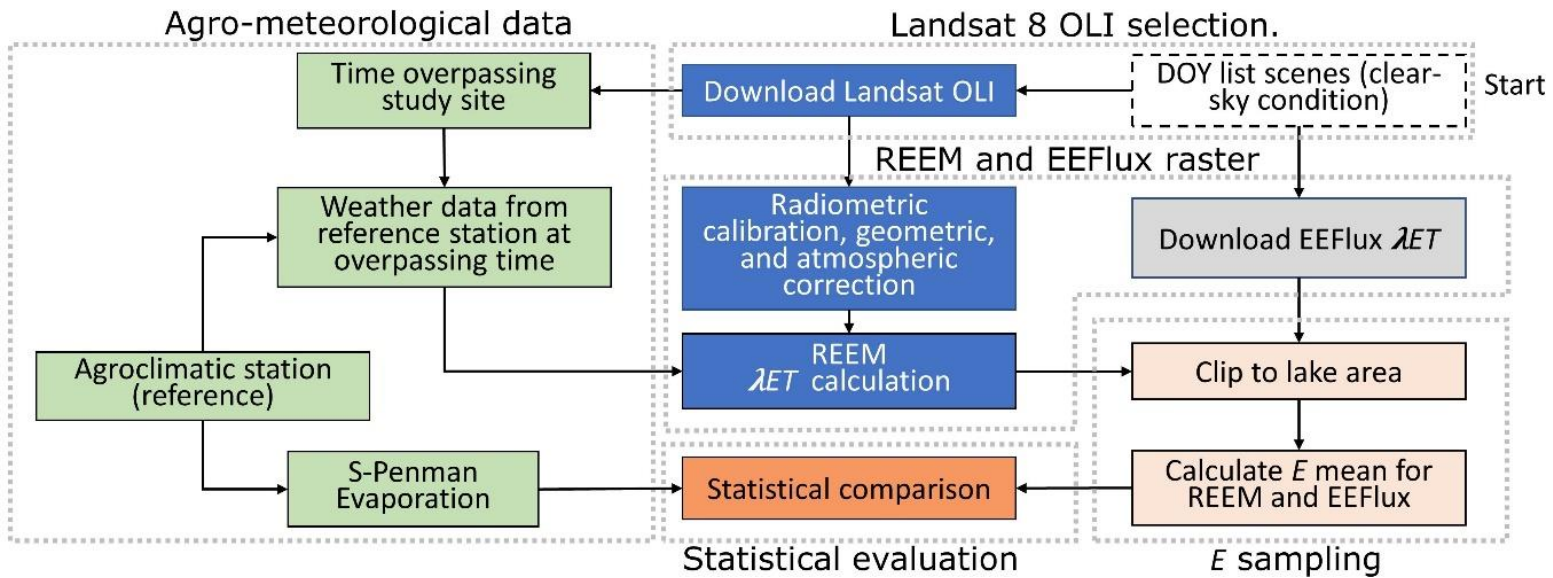
Figure 1. Schematic flow chart comparing the REEM and EEFlux models
to get E estimations by comparing the S-Penman equation.

Study area

This study was conducted during the agricultural cycle from April 2017 to September 2017 in the endorheic basin of Cuauhtemoc Valley. The Bustillos Lake is a shallow freshwater body in the municipality of Cuauhtemoc, Chihuahua, Mexico. The lake is at latitude 28°33'59.36" N and longitude 106°46'7.33" W. The lake has an approximately oval shape, of which the major axis is 17 km, and the minor one is 8 kilometers with

an average depth of 1.7 m. The area can fluctuate around 100 km^2 (Figure 2)(Rojas-Villalobos *et al*., 2018). Currently (August 2019), the surface of Bustillos Lake is 116.7 km^2; moreover, it stores 312.7 hm^3 and has an average depth of 2.68 m. The lake water's turbidity is closely related to the shallow depth and high concentrations of sediment carried by the tributaries. The surface water erosion in the region is mainly due to extensive agriculture, sparse riparian vegetation, and the deforestation of the mountain ranges' slopes that delimit the basin (Álvarez *et al*., 2016; Amado-Alvarez *et al*., 2019).
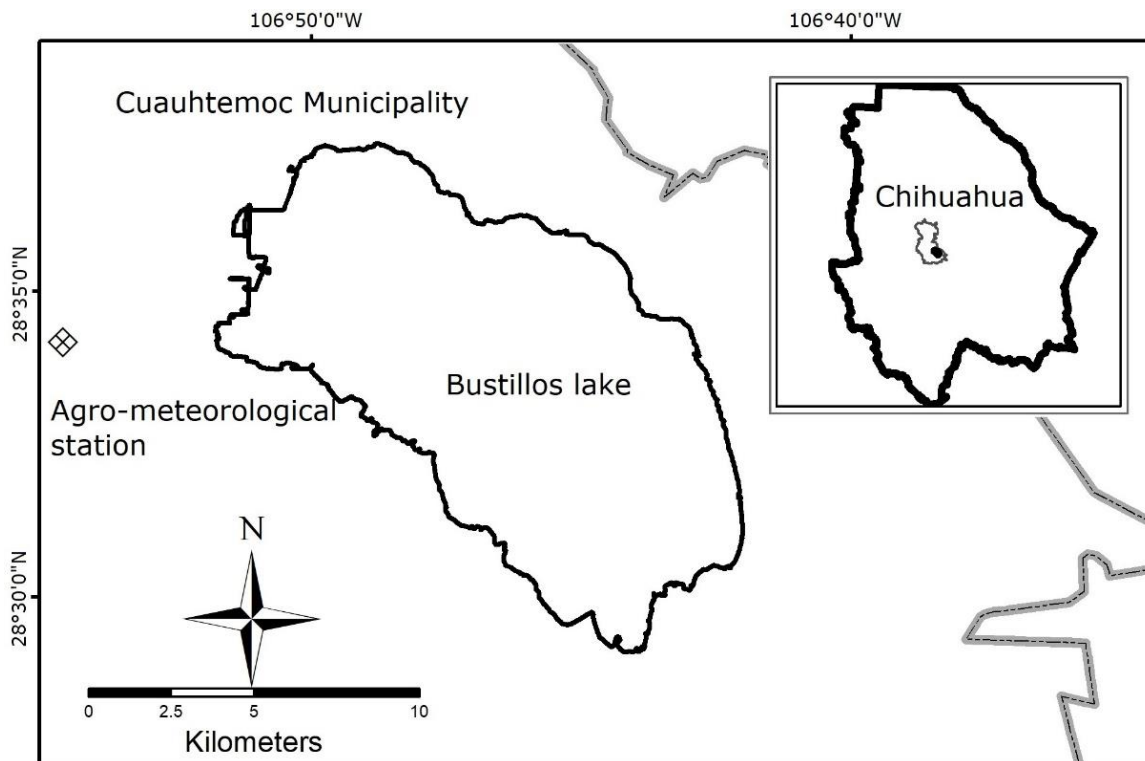

Figure 2. Bustillos Lake location and agrometeorological station. INEGI (2019).

Agro-meteorological data

An agroclimatic station, ADCON™, located 4.5 kilometers west of the Bustillos Lake at 28°34'11.5"N, 106°54'29.4"W, and 2004 m.a.s.l provided hourly meteorological data that REEM required to calculate the ET for each date from downloaded Landsat 8 OLI satellite images. Also, the agroclimatic station provided data for computing E by using the standardized S-Penman equation (Valiantzas, 2006) through TR1 Combi sensors for temperature and relative humidity and pyranometers (SP Lite and CMP3), and wind speed.

Landsat 8 OLI selection

Seven Landsat 8 OLI images (7, 23, and 30 April; 9 and 16 may; 17 july; 14 september) from two different Paths (Path:32,33; Row:40) were chosen for continuity in the temporal and geographical space of the agricultural cycle in the Cuauhtemoc Basin. Additionally, the images met no cloud criteria (clear-sky) in the study area.

REEM and EEFlux raster

The satellite images were radiometrically calibrated and atmospherically corrected using the ENVI® software through the Fast Line-of-sight Atmospheric Analysis of Hypercubes (FLAASH™) tool. Once the satellite images were processed for obtaining the ET_a through the REEM, the ET_a layers of the EEFlux model were downloaded from the web portal (http://eeflux-level1.appspot.com/).

Lake delineation and sampling

The sampling was carried out through a lake polygon that was created using the Modified Normalized Difference Water Index (MNDWI), which discretizes the water surface from the rest of the image (Xu, 2006). The outline of the polygon of the lake was contracted by 50 meters to reduce water detection errors on the shore caused by expanding and contracting throughout the agricultural cycle. One hundred random spatial point

samples were obtained for each day evaluated, for each model compared, giving a total of 700 samples for REEM and 700 samples for EEFLUX.

Statistical evaluation

Statistical comparison was performed using the relationship between the observed values (O_i)(S-PENMAN) and the estimated or predicted values (P_i) (REEM and EEFlux). A set of statistical indicators were applied to evaluate the performance of each model. A linear regression analysis (y=ax+b) was applied to obtain the (a) slopes and (b) interceptions; moreover, a residual analysis was performed to see if there were atypical values that affect the models. According to Chai and Draxler (2014), it is a good practice to include mean absolute error (MAE) and root mean square error (RMSE) because they are indicators that integrate the main differences between observed and estimated values. The variance (S_d^2) was calculated to know how much difference there was between observed and predicted values. The mean bias error (MBE) was included to find if there was a systematic error. The consistent error between the distance of linear regression and the 1:1 line is known as systematic RMSE. Unsystematic RMSE is when the error is randomized, caused by an unknown source. When an unsystematic RMSE has low values, and the systematic RMSE value is close to RMSE, the model can be considered a

good one (Willmott *et al*., 1985). The efficiency model (EF) was applied by using the predicted and observed measured variations (Greenwood, Neeteson, & Draycott, 1985; Nash & Sutcliffe, 1970). Finally, an agreement index (d) (Willmott, 1981, 1982; Willmott & Wicks, 1980) was estimated for comparing hydrological models.

$$MAE = \frac{\sum_{i=1}^{N}|P_i - O_i|}{N} \qquad \text{Lower is better}$$

$$RMSE = \left[\frac{\sum_{i=1}^{N}(P_i - O_i)^2}{N}\right]^{0.5} \qquad \text{Lower is better}$$

$$S_d^2 = \frac{\sum_{i=1}^{N}(P_i - O_i - MBE)^2}{N - 1} \qquad \text{Closer to 0 is better}$$

$$MBE = \frac{\sum_{i=1}^{N}\ (P_i - O_i)}{N} \qquad \text{Closer to 0 is better}$$

$$RMSE_u = \left[\frac{\sum_{i=1}^{N}\left(P_i - \hat{P}_i\right)^2}{N}\right]^{0.5}$$

$$RMSE_s = \left[\frac{\sum_{i=1}^{N}\left(\hat{P}_i - O_i\right)^2}{N}\right]^{0.5}$$

$$EF = 1 - \frac{\sum_{i=1}^{N}(P_i - O_i)^2}{\sum_{i=1}^{N}(\underline{O} - O_i)^2} \qquad (0 \leq EF \leq 1) \text{ closer to 1, better}$$

$$d = 1 - \frac{\sum_{i=1}^{N}(P_i - O_i)^2}{\sum_{i=1}^{N}(|P_i'| - |O_i'|)^2} \qquad (0 \leq EF \leq 1) \text{ closer to 1, better}$$

where O_i +is the observed value (S-Penman) in the record i, P_i is the predicted value from the REEM and EEFlux models in area i, N is the number of observations (7), and n is the number of season days (256). Furthermore, $\widehat{P_i}$, P_i', and O_i' were obtained as

$$\widehat{P_i} = aO_i + b. \qquad P_i' = P_i - \underline{O}. \qquad O_i' = O_i - \underline{O}.$$

Results

The plotted E (S-Penman) results, mean E from the REEM, and the EEFlux for the Bustillos Lake are shown in Figure 3. Table 1 showed EEFlux had significant variations at the beginning of the season on April 7 and April 23 (24.2% and -51.8%, respectively), as well as at the end of the cycle

on June 17 and September 14 (-36.7% and -74.2%), while the REEM had sensitive variations on September 14 (13.6%). In the REEM case, the percentage variations represented a difference of less than 0.7 mm of evaporation except May 9 and June 17, which were 0.98 and 1.11 mm, respectively. The EEFlux presented variations greater than 3.1 mm of evaporation for 3 of the seven days. On April 7, April 30, May 9, and May 16, the models tested variations between the reference model's 1.15 and 1.57 mm.
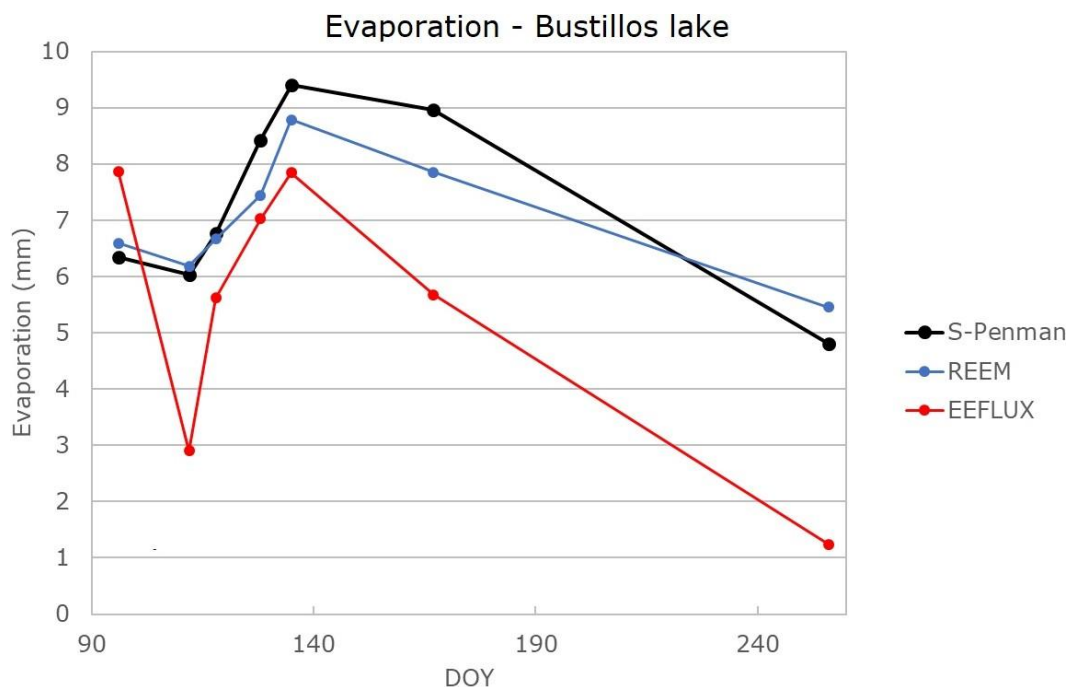

Figure 3. Mean evaporation values of S-Penman, REEM, and EEFlux during the 2017 agricultural season for the Bustillos Lake. Data retrieved from UNIFRUT (2019), USGS LandsatLook Viewer (2019), and EEFlux (2019).

Table 1. Comparative table of errors between the reference evaporation and the models based on remote sensors (REEM and EEFlux).

Date	DOY	E Reference (mm)	REEM		EEFlux	
			mm	Error (%)	mm	Error (%)
7-Apr-2017	96	6.3	6.6	4.0	7.9	24.2
23-Apr-2017	112	6.0	6.2	2.4	2.9	-51.8
30-Apr-2017	118	6.8	6.7	-1.5	5.6	-16.9
9-May-2017	128	8.4	7.4	-11.6	7.0	-16.5
16-May-2017	135	9.4	8.8	-6.6	7.8	-16.6
17-Jun-2017	167	9.0	7.9	-12.3	5.7	-36.7
14-Sep2017	256	4.8	5.5	13.6	1.2	-74.2
Average				-1.7		-26.9

Although the coefficient of determination (R^2) was relatively high (0.953) to indicate that the REEM model produces evaporation values close to observed ones, the slope (a = 0.6374) of the regression line does not ensure continuous linearity of predictions with the reference line (Figure 4a). The interception coefficient (b=2.3779) indicates overestimation data over observed values. In Figure 4b, the slope of the EEFlux (a=1.057) regression line closely matches the 1:1 reference of the observed data (S-Penman). Furthermore, the interception coefficient is negative (b = -2.2123), and R^2 is low (0.5105), which suggests an underestimation and high variance of the values predicted by the model.

Both models concentrate on underestimating and overestimating values (EEFlux and REEM, respectively) in the range of 4.9 to 6.2 mm of daily evaporation.
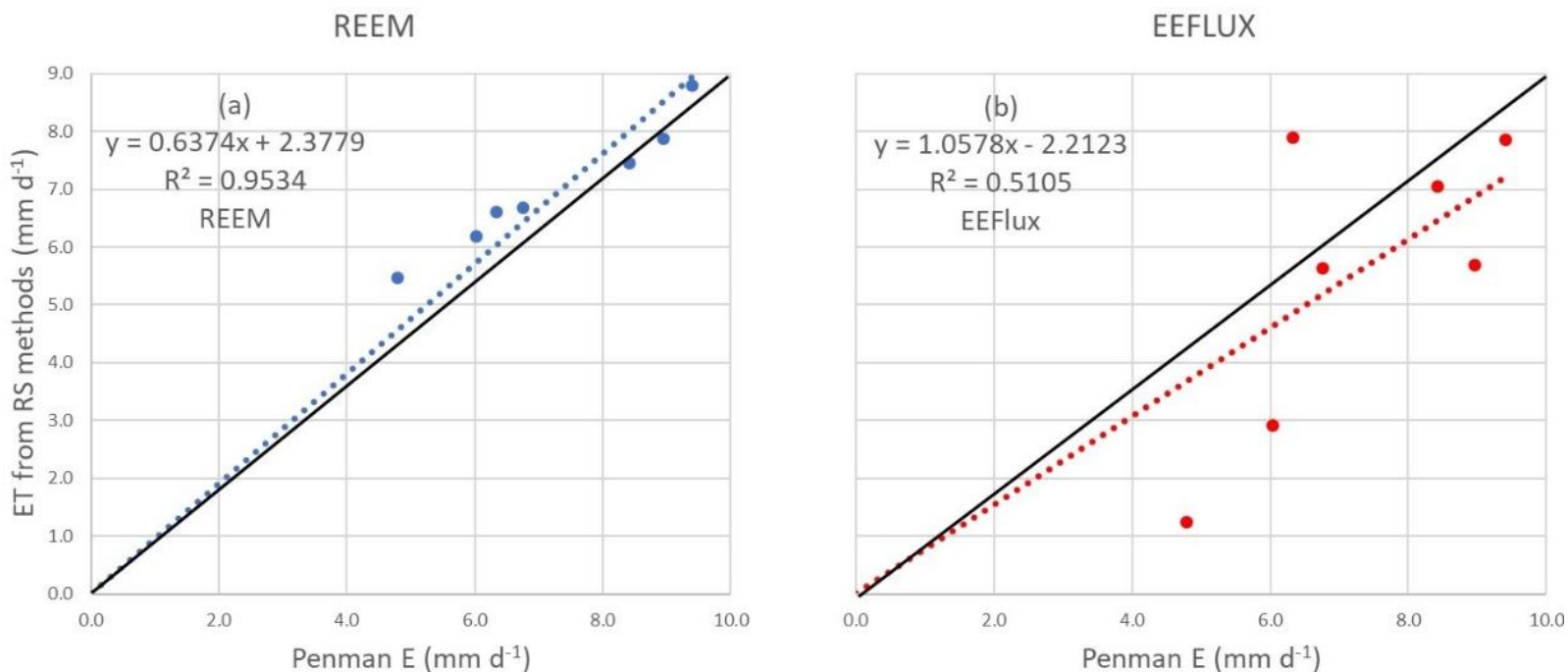

Figure 4. Comparison of the daily reference E (S-Penman) values and the values obtained from RS-based methods: a) REEM and b) EEFlux).

Figure 5 shows that the EEFlux model's variance is not constant: while predicted evaporation values were low, the residual values were atypically high. In the residual analysis, evaporation is related to time. In other words, in April and September, the net radiation and temperatures were low, and as a result, there was less evaporation than that determined between May and August. When comparing the residuals

between the two ET models, the REEM errors concentrate on the strip of ±0.55 mm, which is quite acceptable. In contrast, more than 50% of the EEFlux residuals approximately exceed the range of ±1.37 mm and ±3.5 mm.
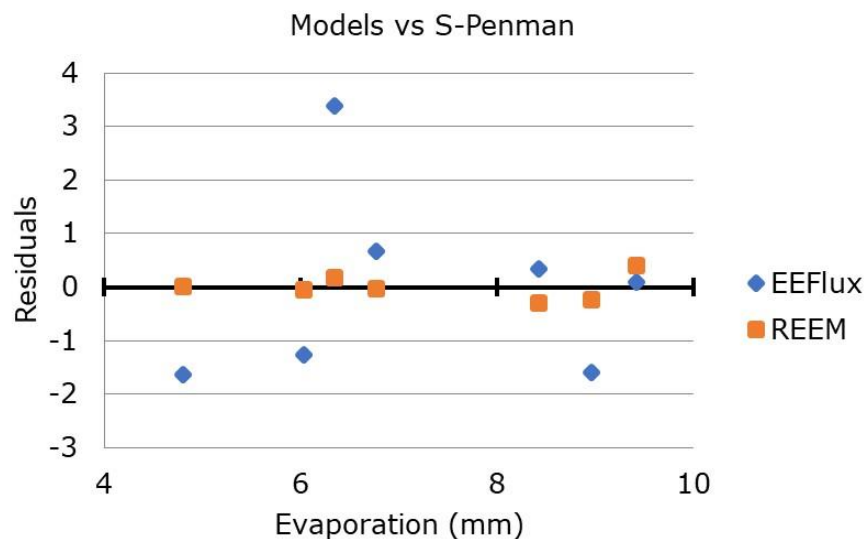

Figure 5. Comparative graphic of residuals predicted E on RS map models versus observed E (S-Penman).

The regression and residual analysis did not provide enough information to measure and compare the models studied. A more in-depth analysis was required for determining substantial differences between the comparison of the data of the predictive models with the reference ones.

Table 2 shows the ranked analytical results for comparing the performance of ET models. For statistical indexes in complex evaluation systems, a weighting coefficient separately calculated is required.

Table 2. Summary of the ranked results of the comparative statistical indicators applied to the REEM and EEFlux versus S-Penman.

Index		REEM (rank)	EEFlux (rank)
MAE	(mm d^{-1})	0.55 (1)	2.23 (2)
RMSE	(mm d^{-1})	-0.66 (1)	2.43 (2)
S$_d^2$	(mm d^{-1})	0.44 (1)	3.14 (2)
MBE	(mm d^{-1})	-0.25 (1)	-1.79 (2)
RMSE$_u$	(mm d^{-1})	0.60 (1)	4.26 (2)
RMSE$_s$	(mm d^{-1})	0.41 (1)	2.14 (2)
EF		0.82(1)	-1.36 (2)
R^2		0.95 (1)	0.51 (2)
d		0.94 (1)	0.68 (2)
a (intercept)		1.75 (2)	1.62 (1)
b (slope)		0.79 (2)	1.07 (1)

The RMSE is criticized for being inappropriate and misinterpreted in environmental and climate analyses (Willmott & Matsuura, 2005). However, the RMSE and MAE results enrich the interpretation of the evaluated models (Chai & Draxler, 2014). In this study, the MAE and RMSE indicators agreed that the REEM presented a lower average error (MAE = 0.55 and RMSE = -0.66 both in mm d^{-1}) among the data. S$_d^2$ confirms the high variability that the EEFlux had (3.14 mm) in predicting the daily ET$_a$ compared to the REEM (0.44 mm). The bias indicator (MBE)

agreed with the initial linear regression analysis as it showed a slight underestimation of the REEM (-0.25 mm) in comparison with the higher underestimation of the values predicted by the EEFlux (-1.79 mm).

The RMSE$_u$ results suggested that an unknown source's noise promoted a poor EEFlux model's performance (4.26 mm). In contrast, the same index showed a lower influence of unknown variables in the REEM model (0.60 mm). EF index values close to 1 correspond to a model that predicts values close to the observed data. If the index is less than 0, the mean observed data is a better predictor than the values estimated from the ET model (Nash & Sutcliffe, 1970; Pushpalatha, Perrin, Moine, & Andréassian, 2012). Therefore, according to the above, the REEM (EF=0.82) had a higher performance than the EEFlux (EF= -1.36). The statistical indicator of agreement "d" indicates the tendency of the previous indexes by suggesting that the REEM (0.94) is a better predictor of ET$_a$ than the EEFlux (0.68). The total E for the three models in the agricultural reference season was compared using daily estimations. In the REEM and EEFlux, a linear interpolation technique was used to calculate the E between the seven available satellite images' dates. The meteorological records of the aforementioned agroclimatic station were used for the computation of the daily E-reference through the S-Penman equation (Figure 6). The variability (SEE) was 3.2 and 3.4 mm day^{-1} for REEM and EEFlux, respectively. The total E for S-Penman was 968 mm, and 1 137 mm for REEM, with 752 mm for EEFlux, equivalent to 115.29, 135.35, and 752 hm^3 of water, respectively.
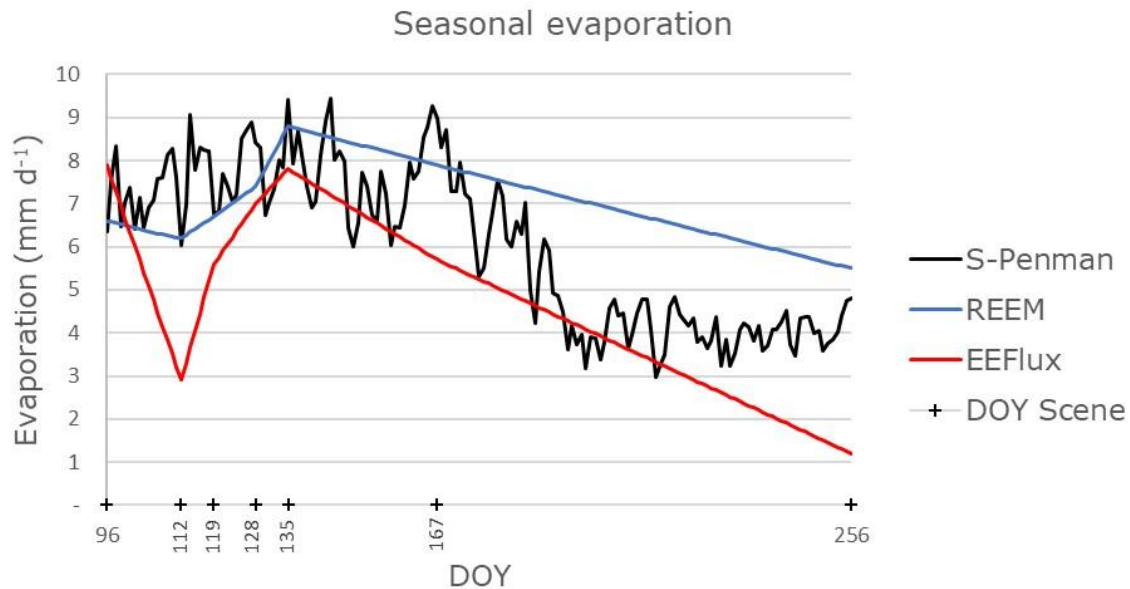
Figure 6. Seasonal evaporation comparison of RS models versus S-Penman data from April 4, 2017 to September 14, 2017.

The residue analysis showed more considerable variability in the low ranges of E reference. Figure 7 displays an ET (out of the lake) and E (over the lake) comparison map of the REEM and EEFlux from agricultural fields and the Bustillos Lake (dated June 17, 2017).
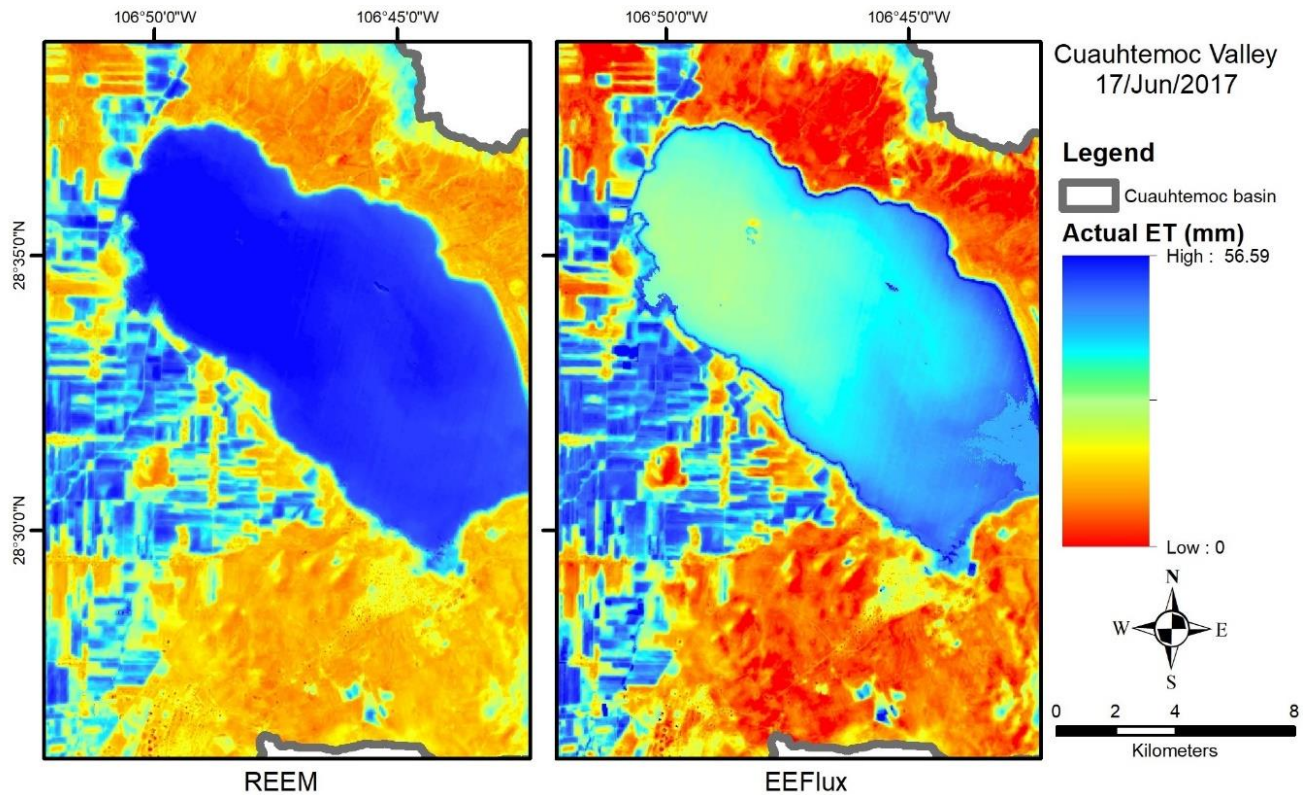
Figure 7. ET (crop fields) and evaporation (lake) comparison maps of REEM and EEFlux models in the Cuauhtemoc Valley for June 17, 2017. Data retrieved from USGS (2019) and EEFlux (2019)**.**

The daily evaporation variability of the RS models and the value measured in the season was high since the variation coefficient was 53.6% for REEM and 55.7% for EEFlux. The daily E variability between the RS models and the value measured in the season was high since the variation coefficient was 53.6 % for REEM and 55.7% for EEFlux. Similarly, the REEM overestimated E by 17.4 % compared to reference values, while EEFlux underestimated E by 22.3% for the same period.

There were significant differences in the coefficients of variation in the segment from May 16 to September 14 (135-256 DOY) when REEM obtained 70% and EEFlux 46%. The differences between the predicted values and the observed values were high because of the large gaps between the acquired satellite images' dates.

Conclusions

Alternative methods to estimate water bodies' evaporation in endorheic basins are very important to monitor the water balance, and even more where monitoring instrumentation is lacking. Therefore, knowing this variable allows establishing policies for the rationed use of water, promoting the water system's balance and its efficient use. Seven Landsat 8 images were used during the agricultural cycle from April to September 2017, when the REEM and EEFlux evapotranspiration models were compared with the reference ET to estimate the daily evaporation of the Bustillos Lake. ET estimation methods by remote sensors are sensitive to variations in weather conditions. In the interpolated grid of climatic parameters, there are regions where there are significant differences between observed and interpolated data. These regions are far from the interpolation source points, and the physical-environmental conditions are

different. Gridded data should aggregate additional data source points where there are significant variations of the climatic parameters. An anchor weather station can improve the predictions of the evaporation of a water body as observed in the REEM model. The location of the weather station is a determining factor in the computation of the ET. In this study, an agroclimatic station located 4.5 km from the Bustillos Lake recorded weather conditions where the prevailing winds (SW-NW) pass before reaching the lake, which establishes the physical conditions for water evaporation. The temporal resolution of the satellite scenes is a determining factor for estimating the total E since the gap between the dates of the images reduces data time uncertainty to obtain accurate values and better performance of the RS models through interpolation methods.

Acknowledgments

References

AghaKouchak, A., Norouzi, H., Madani, K., Mirchi, A., Azarderakhsh, M., Nazemi, A., … Hasanzadeh, E. (2015). Aral Sea syndrome desiccates Lake Urmia: Call for action. *Journal of Great Lakes*

Research, 41(1), 307–311. doi: https://doi.org/10.1016/j.jglr.2014.12.007

Allen, R. G., Morton, C., Kamble, B., Kilic, A., Huntington, J., Thau, D., … Robison, C. (2015). EEFlux: A Landsat-based Evapotranspiration mapping tool on the Google Earth Engine. *2015 ASABE / IA Irrigation Symposium: Emerging Technologies for Sustainable Irrigation - A Tribute to the Career of Terry Howell, Sr. Conference Proceedings*, 1–11. doi: https://doi.org/10.13031/irrig.20152143511

Allen, R. G., Tasumi, M., & Trezza, R. (2007a). *Satellite-Based Energy Balance for Mapping Evapotranspiration with Internalized Calibration (METRIC)-Model*. *133*(4), 135–139. doi: https://doi.org/10.1061/(ASCE)0733-9437(2007)133:4(380)

Allen, R. G., Tasumi, M., Trezza, R., Wright, J. L., Bastiaanssen, W., Kramber, W. J., … Robison, C. (2007b). Satellite-Based Energy Balance for Mapping Evapotranspiration with Internalized Calibration (METRIC)—Applications. *Journal of Irrigation and Drainage Engineering*, 133(4), 395–406. doi: https://doi.org/10.1061/(ASCE)0733-9437(2007)133:4(395)

Álvarez, J. P. A., Cutillas, P. P., Valle, O. R., & Cabañero, J. J. A. (2016). Water resources degradation in a semiarid environment. Bustillos and Los Mexicanos lakes (Chihuahua, México). *Papeles de Geografía*, (62), 107–118.

Amado-Álvarez, J. P., Pérez Cutillas, P., Ramírez Valle, O., & Alarcón Cabañero, J. J. (2016). *Degradación de los recursos hídricos en un*

ambiente semiárido. Las lagunas de Bustillos y de los Mexicanos (Chihuahua, México). Retrieved from https://digitum.um.es/digitum/handle/10201/51756

Amado-Alvarez, J., Pérez-Cutillas, P., Alatorre-Cejudo, L. C., Ramírez-Valle, O., Segovia-Ortega, E. F., & Alarcón-Cabañero, J. J. (2019). Multispectral analysis to estimate the turbidity as an indicator of the quality of water in reservoirs in Chihuahua State, Mexico. *Revista Geográfica de América Central*, 1(62), 49–77. doi: https://doi.org/10.15359/rgac.62-1.2

ASCE–EWRI. (2005). *The ASCE standardized reference evapotranspiration equation.* Reston, VA: ASCE–EWRI Standardization of Reference Evapotranspiration Task Committee Rep.

Ayyad, S., Al Zayed, I. S., Ha, V. T. T., & Ribbe, L. (2019). The Performance of Satellite-Based Actual Evapotranspiration Products and the Assessment of Irrigation Efficiency in Egypt. *Water*, 11(9), 1913. doi: https://doi.org/10.3390/w11091913

Bastiaanssen, W. G. M. (1995). *Regionalization of surface flux densities and moisture indicators in composite terrain: A remote sensing approach under clear skies in Mediterranean climates* (SC-DLO). Retrieved from https://library.wur.nl/WebQuery/wurpubs/28279

Bastiaanssen, W. G. M., Menenti, M., Feddes, R. A., & Holtslag, A. A. M. (1998). A remote sensing surface energy balance algorithm for land (SEBAL). Part 1. Formulation. *Journal of Hydrology*, *212–213*, 198–212. doi: https://doi.org/10.1016/S0022-1694(98)00253-4

Bastiaanssen, W. G. M., Pelgrum, H., Wang, J., Ma, Y., Moreno, J. F., Roerink, G. J., & Van der Wal, T. (1998). A remote sensing surface energy balance algorithm for land (SEBAL). Part 2: Validation. *Journal of Hydrology*, *212–213*, 213–229. doi: https://doi.org/10.1016/S0022-1694(98)00254-6

Blaney, H. F., & Criddle, W. D. (1957). *Determining consumptive use and irrigation water requirements* (Technical Bulletin No. 1275; p. 24). Retrieved from United States Department of Agriculture website: https://naldc.nal.usda.gov/download/CAT87201264/PDF

Bozorgi, A., Bozorg-Haddad, O., Sima, S., & Loáiciga, H. A. (2018). Comparison of methods to calculate evaporation from reservoirs. *International Journal of River Basin Management*, *0*(0), 1–12. doi: https://doi.org/10.1080/15715124.2018.1546729

Brutsaert, W., & Stricker, H. (1979). An advection-aridity approach to estimate actual regional evapotranspiration. *Water Resources Research*, *15*(2), 443–450. doi: https://doi.org/10.1029/WR015i002p00443

Cabrera, M. C. M., Anache, J. A. A., Youlton, C., & Wendland, E. (2016). *Performance of evaporation estimation methods compared with standard 20 m2 tank*. *20*(10), 874–879. doi: https://doi.org/doi.org/10.1590/1807-1929/agriambi.v20n10p874-879

Chai, T., & Draxler, R. R. (2014). Root mean square error (RMSE) or mean absolute error (MAE)?–Arguments against avoiding RMSE in the

literature. *Geoscientific Model Development*, *7*(3), 1247–1250. doi: https://doi.org/10.5194/gmd-7-1247-2014

Cleugh, H. A., Leuning, R., Mu, Q., & Running, S. W. (2007). Regional evaporation estimates from flux tower and MODIS satellite data. *Remote Sensing of Environment*, *106*(3), 285–304. doi: https://doi.org/10.1016/j.rse.2006.07.007

De Bruin, H. a. R. (1978). A Simple Model for Shallow Lake Evaporation. *Journal of Applied Meteorology*, *17*(8), 1132–1134. doi: https://doi.org/10.1175/1520-0450(1978)017<1132:ASMFSL>2.0.CO;2

De Bruin, H. a. R., & Keijman, J. Q. (1979). The Priestley-Taylor Evaporation Model Applied to a Large, Shallow Lake in the Netherlands. *Journal of Applied Meteorology*, *18*(7), 898–903. doi: https://doi.org/10.1175/1520-0450(1979)018<0898:TPTEMA>2.0.CO;2

Diario Oficial de la Federación. (2015, July 6). *ACUERDO por el que se da a conocer el resultado de los estudios técnicos de aguas nacionales subterráneas del Acuífero Cuauhtémoc, clave 0805, en el Estado de Chihuahua, Región Hidrológico Administrativa Río Bravo.* Retrieved from http://www.dof.gob.mx/nota_detalle.php?codigo=5399497&fecha=06/07/2015

Díaz Caravantes, R. E., Bravo Peña, L. C., Alatorre Cejudo, L. C., & Sánchez Flores, E. (2014). Análisis geoespacial de la interacción entre el uso de suelo y de agua en el área peri-urbana de

Cuauhtémoc, Chihuahua. Un estudio socioambiental en el norte de México. *Investigaciones Geográficas, Boletín Del Instituto de Geografía*, *2014*(83), 116–130. doi: https://doi.org/10.14350/rig.32694

Erickson, A. J., Gulliver, J. S., Hozalski, R. M., Mohseni, O., Nieber, J. L., Wilson, B. N., & Weiss, P. T. (2008). Evaporation and Evapotranspiration | Stormwater Treatment: Assessment and Maintenance. In *Assessment of Stormwater Best Management Practices* (p. 112). Retrieved from https://conservancy.umn.edu/bitstream/handle/11299/181358/cfans_asset_115795.pdf?sequence=1

Fisher, J. B., Melton, F., Middleton, E., Hain, C., Anderson, M., Allen, R., … Wood, E. F. (2018). The future of evapotranspiration: Global requirements for ecosystem functioning, carbon and climate feedbacks, agricultural management, and water resources. *Reviews of Geophysics*, 2618–2626. doi: https://doi.org/10.1002/2016WR020175@10.1002/(ISSN)1944-9208.COMHES1

Fu, G., Charles, S. P., & Yu, J. (2009). A critical overview of pan evaporation trends over the last 50 years. *Climatic Change*, *97*(1), 193. doi: https://doi.org/10.1007/s10584-009-9579-1

Greenwood, D. J., Neeteson, J. J., & Draycott, A. (1985). Response of potatoes to N fertilizer: Dynamic model. *Plant and Soil*, *85*(2), 185–203. doi: https://doi.org/10.1007/BF02139623

Gross, M. (2017). The world's vanishing lakes. *Current Biology*, *27*(2), R43–R46. doi: https://doi.org/10.1016/j.cub.2017.01.008

Hamon, W. R. (1960). *Estimating potential evapotranspiration* (Thesis, Massachusetts Institute of Technology). Retrieved from https://dspace.mit.edu/handle/1721.1/79479

Hewitt, I. C., Fernald, A. G., & Samani, Z. A. (2018). Calculating Field-Scale Evapotranspiration with Closed-Chamber and Remote Sensing Methods. *JAWRA Journal of the American Water Resources Association*, *54*(4), 962–973. doi: https://doi.org/10.1111/1752-1688.12654

Hirschi, M., Michel, D., Lehner, I., & Seneviratne, S. I. (2017). A site-level comparison of lysimeter and eddy covariance flux measurements of evapotranspiration. *Hydrology and Earth System Sciences*, *21*(3), 1809–1825. doi: https://doi.org/10.5194/hess-21-1809-2017

Irmak, A., Allen, R. G., Kjaersgaard, J., Huntington, J., Kamble, B., Trezza, R., & Ratcliffe, I. (2012). Operational Remote Sensing of ET and Challenges. *Evapotranspiration - Remote Sensing and Modeling*. doi: https://doi.org/10.5772/25174

Jensen, M. E., & Haise, H. R. (1963). Estimating Evapotranspiration from Solar Radiation. *Proceedings of the American Society of Civil Engineers, Journal of the Irrigation and Drainage Division*, *89*, 15–41.

Kirk, J. T. (1985). Effects of suspensoids (turbidity) on penetration of solar radiation in aquatic ecosystems. *Hydrobiologia*, *125*(1), 195–208. doi: https://doi.org/10.1007/BF00045935

Kıvrak, C., Bawazir, S., Samani, Z., Steele, C., & Sönmez, B. (2019). Using Plant Phenology and Landsat-8 Satellite Data to Quantify Water Use by Onion Crop in the Mesilla Valley, New Mexico. *International Journal of Crop Science and Technology*, *5*(1), 1–13. doi: https://doi.org/10.26558/ijcst.427945

Li, F., Cao, R., Zhao, Y., Mu, D., Fu, C., & Ping, F. (2017). Remote sensing Penman–Monteith model to estimate catchment evapotranspiration considering the vegetation diversity. *Theoretical and Applied Climatology*, *127*(1), 111–121. doi: https://doi.org/10.1007/s00704-015-1628-2

Makkink, G. F. (1957). Testing the Penman Formula by Means of Lysimeters. *Journal of the Institution of Water Engineers*, (11), 277–288.

Martínez Pérez, J. Á., García-Galiano, S. G., Martin-Gorriz, B., & Baille, A. (2017). Satellite-Based Method for Estimating the Spatial Distribution of Crop Evapotranspiration: Sensitivity to the Priestley-Taylor Coefficient. *Remote Sensing*, *9*(6), 611. doi: https://doi.org/10.3390/rs9060611

Mireles, C., & Mellink, E. (2017). Use of Laguna de Bustillos, Chihuahua, by Waterbirds during the 2011–2012 Wintering Season. *The American Midland Naturalist*, *178*(1), 82–96. doi: https://doi.org/10.1674/0003-0031-178.1.82

Monin, A., & Obukhov, A. (1954). Basic laws of turbulent mixing in the atmosphere near the ground. *Tr. Akad. Nauk SSSR Geofiz. Inst*, *24*(151), 163–187.

Nash, J. E., & Sutcliffe, J. V. (1970). River flow forecasting through conceptual models part I — A discussion of principles. *Journal of Hydrology*, *10*(3), 282–290. doi: https://doi.org/10.1016/0022-1694(70)90255-6

Okpara, U. T., Stringer, L. C., Dougill, A. J., & Bila, M. D. (2015). Conflicts about water in Lake Chad: Are environmental, vulnerability and security issues linked? *Progress in Development Studies*, *15*(4), 308–325. doi: https://doi.org/10.1177/1464993415592738

Papadakis, J. (1965). Potential Evapotranspiration. *Soil Science*, *100*, 76. doi: https://doi.org/10.1097/00010694-196507000-00039

Penman, H. L. (1948). Natural evaporation from open water, bare soil and grass. *Proceedings of the Royal Society of London. Series A. Mathematical and Physical Sciences*, *193*(1032), 120–145. doi: https://doi.org/10.1098/rspa.1948.0037

Priestley, C. H. B., & Taylor, R. J. (1972). On the Assessment of Surface Heat Flux and Evaporation Using Large-Scale Parameters. *Monthly Weather Review*, *100*(2), 81–92. doi: 10.1175/1520-0493(1972)100<0081:OTAOSH>2.3.CO;2

Pushpalatha, R., Perrin, C., Moine, N. L., & Andréassian, V. (2012). A review of efficiency criteria suitable for evaluating low-flow simulations. *Journal of Hydrology*, *420–421*, 171–182. doi: https://doi.org/10.1016/j.jhydrol.2011.11.055

Rayner, D. P. (2007). Wind Run Changes: The Dominant Factor Affecting Pan Evaporation Trends in Australia. *Journal of Climate*, *20*(14), 3379–3394. doi: https://doi.org/10.1175/JCLI4181.1

Reitz, M., Senay, G., & Sanford, W. E. (2017). Combining remote sensing and water-balance evapotranspiration estimates for the conterminous United States. *Remote Sensing*, *9*(12), 117. doi: https://doi.org/10.3390/rs9121181

Rohwer, C. (1931). *Evaporation from free water surfaces* (No. 271; p. 107). Retrieved from United States Department of Agriculture website: https://naldc.nal.usda.gov/download/CAT86200265/PDF

Rojas-Villalobos, H. L., Alatorre-Cejudo, L. C., Stringman, B., Samani, Z., & Brown, C. (2018). Topobathymetric 3D model reconstruction of shallow water bodies through remote sensing, GPS, and bathymetry. *TECNOCIENCIA Chihuahua*, *12*(1), 42–54. doi: https://doi.org/10.5281/zenodo.3341734

Rooney, G. G., & Bornemann, F. J. (2013). The performance of FLake in the Met Office Unified Model. *Tellus A: Dynamic Meteorology and Oceanography*, *65*(1), 21363. doi: https://doi.org/10.3402/tellusa.v65i0.21363

Samani, A., & Bawazir, S. (2015). *Improving evapotranspiration estimation using remote sensing technology* (TECHNICAL COMPLETION REPORT No. 125548; p. 28). Retrieved from https://nmwrri.nmsu.edu/wp-content/SWWA/Reports/Bawazir/June2015FINAL/report.pdf

Samani, Z., Bawazir, A. S., Skaggs, R. K., Bleiweiss, M. P., Piñon, A., & Tran, V. (2007). Water Use by Agricultural Crops and Riparian Vegetation: An Application of Remote Sensing Technology. *Journal*

of Contemporary Water Research & Education, *137*(1), 8–13. doi: https://doi.org/10.1111/j.1936-704X.2007.mp137001002.x

Samani, Z., Bawazir, S., Bleiweiss, M., Skaggs, R., Piñon, A., & Tran, V. D. (2007). Estimating Daily Net Radiation over Vegetation Canopy through Remote Sensing and Climatic Data. *Journal of Irrigation and Drainage Engineering*, *133*(4), 291–297. doi: https://doi.org/10.1061/(ASCE)0733-9437(2007)133:4(291)

Samani, Z., Bawazir, S., Bleiweiss, M., Skaggs, R., & Schmugge, T. (2006). *Estimating riparian ET through remote sensing*. Presented at the AGU Fall Meeting, San Francisco.

Samani, Z., Sammis, T., Skaggs, R., Alkhatiri, N., & Deras, J. (2005). Measuring On-Farm Irrigation Efficiency with Chloride Tracing under Deficit Irrigation. *Journal of Irrigation and Drainage Engineering*, *131*(6), 555–559. doi: https://doi.org/10.1061/(ASCE)0733-9437(2005)131:6(555)

Samani, Z., Skaggs, R., & Bleiweiss, M. (2005). Regional ET Estimation Model, REEM. *Proc. 31st Intl. Symposium on Remote Sensing from Satellite*. Presented at the Proc. 31st Intl. Symposium on Remote Sensing from Satellite, Tucson, AR.

Senkondo, W., Munishi, S. E., Tumbo, M., Nobert, J., & Lyon, S. W. (2019). Comparing Remotely-Sensed Surface Energy Balance Evapotranspiration Estimates in Heterogeneous and Data-Limited Regions: A Case Study of Tanzania's Kilombero Valley. *Remote Sensing*, *11*(11), 1289. doi: https://doi.org/10.3390/rs11111289

Smith, R. C., & Tyler, J. E. (1967). Optical Properties of Clear Natural Water*. *JOSA*, *57*(5), 589–595. doi: 10.1364/JOSA.57.000589

Stephens, J. C., & Stewart, E. H. (1963). *A comparison of procedures for computing evaporation and evapotranspiration* (pp. 123–133). Fort Lauderdle, Florida.

Subin, Z. M., Murphy, L. N., Li, F., Bonfils, C., & Riley, W. J. (2012). Boreal lakes moderate seasonal and diurnal temperature variation and perturb atmospheric circulation: Analyses in the Community Earth System Model 1 (CESM1). *Tellus A: Dynamic Meteorology and Oceanography*, *64*(1), 15639. doi: https://doi.org/10.3402/tellusa.v64i0.15639

UNIFRUT. (2019). Resumen de las estaciones meteorológicas por municipios. Retrieved February 20, 2019, from http://unifrut.com.mx/rem/

Valiantzas, J. D. (2006). Simplified versions for the Penman evaporation equation using routine weather data. *Journal of Hydrology*, *331*(3), 690–702. doi: https://doi.org/10.1016/j.jhydrol.2006.06.012

Yaseen, Z. M., Al-Juboori, A. M., Beyaztas, U., Al-Ansari, N., Chau, K. W., Qi, C., ... & Shahid, S. (2020). Prediction of evaporation in arid and semiarid regions: a comparative study using different machine learning models. *Engineering applications of computational fluid mechanics*, 14(1), 70-89. doi: https://doi.org/10.1080/19942060.2019.1680576